Transformation of Output Constraints in Optimal Control Applied to a Double Pendulum on a Cart

B. Käpernick K. Graichen

Institute of Measurement, Control and Microtechnology, University of Ulm, Germany (e-mail: {bartosz.kaepernick,knut.graichen}@uni-ulm.de).

Abstract: This paper describes a constraint transformation technique for optimal control problems (OCP) with nonlinear single-input single-output (SISO) systems subject to output constraints. An input-output transformation and saturation functions are used to transform the system dynamics into a new unconstrained representation. This method allows to reformulate the original OCP into an unconstrained counterpart. The transformation technique is applied to a double pendulum on a cart in order to compute optimal trajectories for a multi-stage transition scenario. Simulation as well as experimental results with an additional feedback control demonstrate the applicability of the presented method.

Keywords: Optimal control, output constraints, constraint transformation.

1. INTRODUCTION

The interest in optimization methods for control applications has increased over the last decades. This is mainly motivated by the advancement of computational power and the development of efficient techniques and algorithms to solve optimal control problems (OCP). The combination of both of these aspects, namely computational power and efficient algorithms, makes the real-time solution of OCP's possible, as the field of model predictive control (MPC) demonstrates, see e.g. Ohtsuka (2004), Houska et al. (2011).

A common approach to solve optimal control problems is to discretized the OCP, for instance by means of a multiple shooting scheme (Leineweber et al., 2003) or full discretization (Hargraves and Paris, 1987). In this way, the problem is reduced to a nonlinear programming (NLP) problem which can be solved by using sequential quadratic programming (SQP) methods or interior point (IP) methods (Wright, 1997; Nocedal and Wright, 2006).

A more classical way to solve an OCP is to use the calculus of variations, see i.e. Bryson and Ho (1969). This method is based on the necessary optimality conditions forming a two-point boundary value problem (BVP). The main drawback of this method is, however, that state constraints are in general difficult to incorporate due to the occurrence of discontinuities between constrained and unconstrained arcs (Bryson and Ho, 1969), which consequently requires knowledge of the optimal solution.

This paper presents an approach to circumvent this issue in optimal control. In Graichen and Zeitz (2008) a method is presented, how input and output constraints can be incorporated into a new system representation using a normal form transformation and a subsequent replacement of the constraints by means of saturation functions. The approach was originally developed for the inversion-based feedforward control design in the sense of nonlinear control and is extended in this paper to optimal control problems with constraints on the output and a number of its time derivatives. A similar extension can be found in Graichen and Petit (2009) for a class of state constraints but the method is restricted in the sense that the number of incorporated state constraints depends on the number of control inputs. Another technique to account for output constraints while stabilizing a class of nonlinear systems is discussed in Bürger and Guay (2010), where a recursive procedure is used to derive conditions for constraint satisfaction in combination with a suitable switching control law. This paper demonstrates, how more constraints (in form of constraints on the output and a number of its time derivatives) can be taken into account in spite of the presence of a single control input. Problems with this form of constraints are for instance typical in mechanical systems, where the position, the velocity and the acceleration may be limited. After its derivation, the transformation method is applied to compute optimal trajectories for a two-degree-of-freedom control scheme in order to perform a combined swing-up/swing-down and side-step maneuver of a double pendulum on a cart. The applicability and performance are demonstrated in simulation as well as experimentation studies.

2. PROBLEM FORMULATION AND CONSTRAINT TRANSFORMATION

In the following, a transformation technique is presented to incorporate constraints on the output and a number of its time derivatives in optimal control problems. The method to be presented is addressed for the single-input single-output (SISO) case.

2.1 Problem formulation

We consider a nonlinear SISO system

$$\dot{x} = f(x,u)\,, \tag{1a}$$
$$y = h(x) \tag{1b}$$

with state $x \in \mathbb{R}^n$, control $u \in \mathbb{R}$ and output $y \in \mathbb{R}$. The vector field $f : \mathbb{R}^n \times \mathbb{R} \to \mathbb{R}^n$ and the output function $h : \mathbb{R}^n \to \mathbb{R}$ are assumed to be sufficiently smooth. The initial and terminal conditions are given by

$$x(0) = x_0\,, \quad x(T) = x_T\,. \tag{2}$$

The output y and its time derivatives up to order r are subject to the constraints

$$y^{(i)} \in [y_i^-, y_i^+]\,, \quad i = 0,\dots,r\,. \tag{3}$$

The differentiation order r represents the relative degree of (1b) and is defined according to Isidori (1995) [1]

$$\frac{\partial}{\partial u} L_f^j h(x) = 0\,, \quad j = 0,\dots,r-1\,, \quad \frac{\partial}{\partial u} L_f^r h(x) \neq 0 \tag{4}$$

where the expression L_f denotes the Lie derivative along the vector field f. Throughout the paper it is assumed, that the relative degree is well-defined. The cost functional to be minimized is

$$J(u) = V(x(T)) + \int_0^T L(x,u)\,\mathrm{d}t \tag{5}$$

with sufficiently smooth functions $V : \mathbb{R}^n \to \mathbb{R}$ and $L : \mathbb{R}^n \times \mathbb{R} \to \mathbb{R}$. The end time T is fixed.

The problem formulation for this paper can now be summarized in the following optimal control problem:

$$\begin{aligned}
\min_{u(\cdot)} \quad & J(u) = V(x(T)) + \int_0^T L(x,u)\,\mathrm{d}t \\
\text{s.t.} \quad & \dot{x} = f(x,u)\,, \quad y = h(x) \\
& x(0) = x_0\,, \quad x(T) = x_T \\
& y^{(i)} \in [y_i^-, y_i^+]\,, \quad i = 0,\dots,r\,, \quad t \in [0,T]\,.
\end{aligned} \tag{6}$$

In the next section, a constraint transformation that was originally presented for inversion-based feedforward control design in the sense of nonlinear control (Graichen and Zeitz, 2008) is extended to the OCP form (6).

2.2 Transformation into Byrnes-Isidori normal form

The output y of system (1) is used as linearizing output in order to obtain a change of coordinates

$$\begin{bmatrix} y \\ \vdots \\ y^{(r-1)} \\ \eta \end{bmatrix} = \begin{bmatrix} h(x) \\ \vdots \\ L_f^{r-1} h(x) \\ \theta_z(x) \end{bmatrix} = \theta(x) \tag{7a}$$

with the corresponding inverse relation

$$x = \theta^{-1}(y,\dots,y^{(r-1)},\eta)\,. \tag{7b}$$

The arbitrary coordinates $\eta \in \mathbb{R}^{n-r}$ are required to complete the diffeomorphism (7a) for a relative degree $r < n$. By means of (7a), system (1) can be transformed into the Byrnes-Isidori normal form (Isidori, 1995)

$$y^{(r)} = a(y,\dots,y^{(r-1)},\eta,u) \tag{8a}$$
$$\dot{\eta} = b(y,\dots,y^{(r-1)},\eta,u) \tag{8b}$$

with $a = L_f^r h(x) \circ \theta^{-1}$ and $b = L_f \theta_\eta \circ \theta^{-1}$. The chain of integrators (8a) correspond to the input-output dynamics and (8b) represents the internal dynamics with respect to the output (1b). The constraints (3) now act along the states of the cascade (8a).

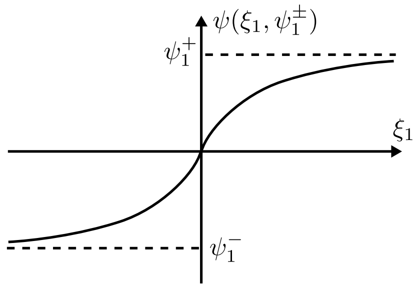

Fig. 1. Asymptotic saturation function $\psi_1(\xi_1, \psi_1^\pm)$ with saturation limits $\psi_1^\pm$.

2.3 Introduction of saturation functions

The constraints (3) can be accounted for by successively introducing saturation functions and differentiating the output y. In the first step, the output is replaced by a saturation function of the form

$$y = \psi_1(\xi_1, \psi_1^\pm) \in (\psi_1^-\,,\, \psi_1^+) \tag{9}$$

with the new unconstrained variable $\xi_1 \in \mathbb{R}$ and the saturation limits $\psi_1^\pm = y_0^\pm$ in order to fulfill the constraint $y \in [y_0^-, y_0^+]$. Note that $\psi_1(\xi_1, \psi_1^\pm)$ is assumed to be strictly monotonically increasing (i.e. $\partial\psi_1/\partial\xi_1 > 0$) and asymptotic in the sense that $\psi_1 \to \psi_1^\pm$ for $\xi_1 \to \pm\infty$, as it is illustrated in Fig. 1.

Equation (9) is now differentiated by means of the chain rule [2]

$$\dot{y} = \frac{\partial\psi_1}{\partial\xi_1}\dot{\xi}_1\,, \tag{10}$$

where the resulting time derivative $\dot{\xi}_1$ has to be chosen such that the constraint $\dot{y} \in [y_1^-\,,\, y_1^+]$ is fulfilled. This can be achieved by introducing a second saturation function

$$\dot{\xi}_1 = \psi_2(\xi_2, \psi_2^\pm) \in (\psi_2^-, \psi_2^+) \tag{11}$$

with a new unconstrained coordinate $\xi_2 \in \mathbb{R}$ and appropriate saturation limits $\psi_2^\pm$. In view of (10) and (11) as well as the constraint $\dot{y} \in [y_1^-\,,\, y_1^+]$, the following inequality must be fulfilled

$$y_1^- \le \frac{\partial\psi_1}{\partial\xi_1}\psi_2(\xi_2, \psi_2^\pm) \le y_1^+\,. \tag{12}$$

Dividing (12) by the partial derivative $\partial\psi_1/\partial\xi_1$ directly leads to the saturation limits

$$\psi_2^\pm(\xi_1) = \frac{y_1^\pm}{\frac{\partial\psi_1}{\partial\xi_1}}\,. \tag{13}$$

Note that the strict monotonicity of the saturation functions ($\partial\psi_1/\partial\xi_1 > 0$) ensures the boundedness of $\psi_2^\pm$. Moreover, the saturation limits (13) do not only depend on $y_1^\pm$ but also on the previously introduced coordinate ξ_1. Hence, the saturation limits are not constant.

[1] The definition of the relative degree is adapted in this paper for general nonlinear systems (1a).

[2] In the following lines, the function arguments are omitted where it is convenient to maintain readability.

The approach of differentiating (9) and introducing saturation functions to account for the constraints (3) leads to the general expression for the output derivatives

$$y^{(i)} = \gamma_i(\xi_1, \dots, \xi_i) + \prod_{j=1}^{i} \frac{\partial \psi_j}{\partial \xi_j} \dot{\xi}_i \,, \quad i = 1, \dots, r \tag{14}$$

with the nonlinear functions $\gamma_i(\cdot)$ involving higher derivatives of the saturation functions. During each differentiation, a further saturation function is introduced for $\dot{\xi}_i$ leading to a new dynamical system of the form

$$\begin{aligned} \dot{\xi}_1 &= \psi_2(\xi_2, \psi_2^{\pm}(\xi_1)) \\ &\vdots \\ \dot{\xi}_{r-1} &= \psi_r(\xi_r, \psi_r^{\pm}(\xi_1, \dots, \xi_{r-1})) \\ \dot{\xi}_r &= \psi_{r+1}(v, \psi_{r+1}^{\pm}(\xi)) \end{aligned} \tag{15}$$

where $v \in \mathbb{R}$ serves as new unconstrained input and $\xi = [\xi_1, \dots, \xi_r]^\mathsf{T}$ comprises all variables ξ_i. The input-output dynamics (8a) can now be replaced by the new dynamics (15).

The general form of the output derivative (14) can be used to determine the saturation limits $\psi_i^{\pm}$, $i = 2, \dots, r+1$, such that the constraints $y^{(i)} \in [y_i^-, y_i^+]$ are fulfilled. To this end, the inequality

$$y_i^- \leq \gamma_i(\xi_1, \dots, \xi_i) + \prod_{j=1}^{i} \frac{\partial \psi_j}{\partial \xi_j} \psi_{i+1}(\cdot, \psi_{i+1}^{\pm}(\xi_1, \dots, \xi_i)) \leq y_i^+ \tag{16}$$

must be satisfied for all $i = 1, \dots, r$, which directly yield the saturation limits

$$\psi_{i+1}^{\pm}(\xi_1, \dots, \xi_i) = \frac{y_i^{\pm} - \gamma_i(\xi_1, \dots, \xi_i)}{\prod_{j=1}^{i} \frac{\partial \psi_j}{\partial \xi_j}} \,. \tag{17}$$

The argument in $\psi_{i+1}(\cdot, \psi_{i+1}^{\pm}(\xi_1, \dots, \xi_i))$ is either the variable ξ_{i+1} or the new input v for $i = r$. Note that the saturation limits $\psi_{i+1}^{\pm}$ of every new saturation function ψ_{i+1} depend on the previous variables $\xi_1, \dots, \xi_i$.

The procedure described above provides a change of coordinates between the constrained output y and its $r-1$ time derivatives and the unconstrained variables $\xi = [\xi_1, \dots, \xi_r]^\mathsf{T}$ according to

$$[y, \dot{y}, \dots, y^{(r-1)}]^\mathsf{T} = h_y(\xi) \tag{18}$$

where $h_y(\xi)$ comprises the saturation function (9) and the nonlinear relations (14) for $i = 1, \dots, r-1$.

Remark 1. A suitable choice for $\psi_i(\xi_i, \psi_i^{\pm})$ is

$$\psi_i(\xi_i, \psi_i^{\pm}) := \psi_i^+ - \frac{\psi_i^+ - \psi_i^-}{1 + \exp\left(\frac{4\xi_i}{\psi_i^+ - \psi_i^-}\right)} \tag{19}$$

with the normalized slope $\psi_i'(0, \psi_i^{\pm}) = 1$. The last saturation function with argument v is defined appropriately.

2.4 New unconstrained problem formulation

The transformation into Byrnes-Isidori normal form and the successive incorporation of the constraints lead to an overall transformation between the original variables x and u and the new unconstrained ones $\bar{x}^\mathsf{T} = [\xi^\mathsf{T}, \eta^\mathsf{T}]$ and v according to

$$\begin{aligned} x &\overset{(7\text{b},18)}{=} \theta^{-1}(h_y(\xi), \eta) &&=: h_x(\bar{x}) \\ u &\overset{(8\text{a})}{=} a^{-1}(y, \dots, y^{(r)}, \eta) &&\overset{(18,14)}{=:} h_u(\bar{x}, v) \,. \end{aligned} \tag{20}$$

Note that the inverse relations

$$\bar{x} = \begin{bmatrix} \xi \\ \eta \end{bmatrix} = h_x^{-1}(x) \,, \quad v = h_u^{-1}(h_x^{-1}(x), u) \tag{21}$$

are only defined on the open intervals of the constraints $y^{(i)} \in (y_i^-, y_i^+)$, $i = 0, \dots, r$ due to the asymptotic behavior of the saturation functions.

The original system dynamics (1a) is replaced by the new system representation in the new variables $\bar{x}$ with the new control v according to

$$\left.\begin{aligned} \dot{\xi}_1 &= \psi_2(\xi_2, \psi_2^{\pm}(\xi_1)) \\ &\vdots \\ \dot{\xi}_r &= \psi_{r+1}(v, \psi_{r+1}^{\pm}(\xi)) \\ \dot{\eta} &= \bar{b}(\xi, \eta, v) \end{aligned}\right\} \quad \dot{\bar{x}} = \bar{f}(\bar{x}, v) \tag{22}$$

where $\bar{b} = b \circ h_y \circ h_u$ denotes the substituted internal dynamics following from (8b).

As the outcome of the transformation procedure, the optimal control problem (6) given in Section 2.1 is now reformulated by means of the coordinate transformation (20) and the new dynamics (22). A new unconstrained OCP can then be stated according to

$$\begin{aligned} \min_{v(\cdot)} \quad & \bar{J}(v) = \bar{V}(\bar{x}(T)) + \int_0^T \bar{L}(\bar{x}, v) + \varepsilon v^2 \, \mathrm{d}t \\ \text{s.t.} \quad & \dot{\bar{x}} = \bar{f}(\bar{x}, v) \\ & \bar{x}(0) = h_x^{-1}(x_0) \,, \; x(T) = h_x^{-1}(x_T) \,, \; t \in [0, T] \end{aligned} \tag{23}$$

with $\bar{V} = V \circ h_x$ and $\bar{L} = L \circ h_x \circ h_u$. OCP (23) is fully unconstrained since the constraints are incorporated in the dynamics (22).

Compared to the original cost (6), the integral cost of problem (23) contains a regularization term εv^2 for some regularization parameter $\varepsilon > 0$. A deeper look at the optimality conditions reveals that a constrained arc of the original OCP (6) corresponds to a singular arc of OCP (23). This effect is counteracted by adding the regularization term. In practice, OCP (23) is solved with decreasing values of $\varepsilon \to 0$. More details on the regularization term and convergence properties of (23) for another class of constraints are discussed in Graichen and Petit (2009).

3. OPTIMAL CONTROL OF A DOUBLE PENDULUM ON A CART

The constraint transformation is illustrated for a nonlinear model of a double pendulum on a cart in order to compute optimal trajectories for a constrained swing-up and side-step maneuver. The obtained trajectories are used in a two-degree-of-freedom control scheme for an experimental setup. The achieved simulation and experimental results are discussed in this section to demonstrate the applicability of the presented approach.

3.1 Problem formulation and system dynamics

The double pendulum consists of two connected links mounted on a cart, see Fig. 2. Each link has a length l_i

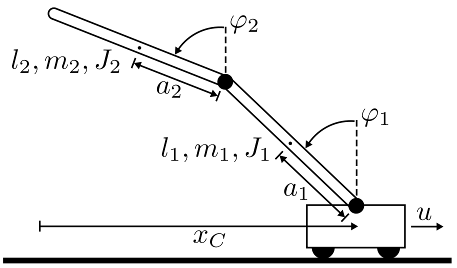

Fig. 2. Schematic of the double pendulum on a cart with mechanical parameters.

and a mass m_i and describes an angle φ_i to the vertical. The center of mass for both links is denoted by a_i and the corresponding moment of inertia is J_i. The measured and identified mechanical parameters for an experimental setup of the double pendulum are descibed in Table 1.

The cart dynamics describes a simple double integrator where the cart displacement $x_1 = x_C$ and the velocity $x_2 = \dot{x}_C$ serve as states. Moreover, the acceleration of the cart is used as control, i.e. $u = \ddot{x}_C$. On the other hand, the system dynamics of the double pendulum can be derived via the Lagrangian method. The corresponding states are the angles φ_i and the angular rates $\dot{\varphi}_i$, i.e. $x_3 = \varphi_1$, $x_4 = \dot{\varphi}_1$, $x_5 = \varphi_2$ and $x_6 = \dot{\varphi}_2$. The combination of both dynamics then leads to the following system representation

$$\left.\begin{array}{ll} \dot{x}_1 = x_2, & \dot{x}_2 = u \\ \dot{x}_3 = x_4, & \dot{x}_4 = f_{\varphi_1}(x_3, \ldots, x_6, u) \\ \dot{x}_5 = x_6, & \dot{x}_6 = f_{\varphi_2}(x_3, \ldots, x_6, u) \end{array}\right\} \; \dot{x} = f(x, u) \quad (24a)$$

$$y = x_1 \,. \quad (24b)$$

A detailed derivation for the nonlinear functions f_{φ_i} can be found in Graichen et al. (2007) and is omitted here due to the lack of space. In addition, the cart displacement is chosen as output (cf. (24b)) in order to account for the constraints

$$y \in [y_0^-, y_0^+], \quad \dot{y} \in [y_1^-, y_1^+], \quad \ddot{y} \in [y_2^-, y_2^+] \,. \quad (25)$$

In this regard, it directly follows in view of the double integrator in (24a) that the relative degree is $r = 2$ and is well-defined for all $x \in \mathbb{R}^6$.

The control task is to perform a set of setpoint changes. To this end, the required feedforward control is computed by solving the following OCP:

$$\begin{aligned} \min_{u(\cdot)} \quad & J(u) = \int_0^T \Delta x^\mathsf{T} Q \Delta x + R \Delta u^2 \, \mathrm{d}t \\ \text{s.t.} \quad & \dot{x} = f(x, u) \,, \quad y = x_1 \qquad (26) \\ & x(0) = x_0 \,, \quad x(T) = x_T \\ & y^{(i)} \in [y_i^-, y_i^-] \,, \quad i = \{0, 1, 2\} \,, \quad t \in [0, T] \end{aligned}$$

Table 1. Mechanical parameters of the double pendulum.

Mechanical parameter	link 1 ($i = 1$)	link 2 ($i = 2$)
length l_i [m]	0.3220	0.4830
center of mass a_i [m]	0.1914	0.2081
mass m_i [kg]	0.6971	0.4418
moment of inertia J_i [N m s^2]	0.0107	0.0164
friction constant d_i [N m s]	0.0000	0.0025

where $Q \in \mathbb{R}^{n \times n}$ is a positive semi-definite matrix, $R \in \mathbb{R}$ is a strictly positive scalar and $\Delta x = x - x_{SP}$ and $\Delta u = u - u_{SP}$ denote the distance to a desired setpoint.

In Graichen et al. (2007) a swing-up maneuver of the double pendulum without direct incorporation of constraints is demonstrated. Thereby, an inversion-based feedforward control design was used to compute the required trajectories. In this paper, the constraints (25) are directly considered via the OCP (26) to calculate optimal trajectories for a combined swing-up/swing-down and side-step action of the double pendulum.

3.2 Transformation into unconstrained problem

Byrnes-Isidori normal form Following the approach discussed in Section 2, the system (24) is first transformed into Byrnes-Isidori normal form with respect to the output y. As mentioned before, the relative degree is $r = 2$ and a simple change of coordinates is (cf. (7a))

$$[y, \dot{y}]^\mathsf{T} = [x_1, x_2]^\mathsf{T} \quad (27a)$$

$$\eta = [\eta_1, \ldots, \eta_4]^\mathsf{T} = [x_3, x_4, x_5, x_6]^\mathsf{T} . \quad (27b)$$

Obviously, the system (24) is already in Byrnes-Isidori normal form with input-output dynamics (corresponds to the double integrator) and internal dynamics (represented by the pendulum dynamics). Therefore, the formulation of system (8) is omitted for the sake of space.

Introduction of saturation functions The output constraint $y \in [y_0^-, y_0^+]$ is first substituted by introducing the saturation function

$$y = \psi_1(\xi_1, \psi_1^\pm) \quad (28)$$

with the saturation limits $\psi_1^\pm = y_0^\pm$. Then (28) is differentiated with respect to time which yields

$$\dot{y} = \frac{\partial \psi_1}{\partial \xi_1} \underbrace{\psi_2(\xi_2, \psi_2^\pm)}_{=\dot{\xi}_1} \quad (29)$$

where the derivative $\dot{\xi}_1$ is replaced in order take the constraint $\dot{y} \in [y_1^-, y_1^+]$ into account. In view of the general formulation (17) for the saturation limits, $\psi_2^\pm$ are computed by the relation

$$\psi_2^\pm = \frac{y_1^\pm}{\frac{\partial \psi_1}{\partial \xi_1}} . \quad (30)$$

A final differentiation of (29) and introduction of another saturation function for the last constraints lead to

$$\ddot{y} = u = \underbrace{\frac{\partial^2 \psi_1}{\partial \xi_1^2} \psi_2^2 + \frac{\partial \psi_1}{\partial \xi_1} \frac{\partial \psi_2}{\partial \xi_1} \psi_2}_{=\gamma_2(\xi)} + \frac{\partial \psi_1}{\partial \xi_1} \frac{\partial \psi_2}{\partial \xi_2} \psi_3(v, \psi_3^\pm) \quad (31)$$

with $\xi = [\xi_1, \xi_2]^\mathsf{T}$, the new input v and the limits

$$\psi_3^\pm = \frac{y_2^\pm - \gamma_2(\xi)}{\frac{\partial \psi_1}{\partial \xi_1} \frac{\partial \psi_2}{\partial \xi_2}} \,. \quad (32)$$

The overall change of variables (20) between (x, u) and $(\bar{x}, v) = (\xi, \eta, v)$ is

$$
\begin{aligned}
x = h_x(\bar{x}) \quad &= \begin{bmatrix} \psi_1(\xi_1, \psi_1^{\pm}) \\ \dfrac{\partial \psi_1}{\partial \xi_1} \psi_2(\xi_2, \psi_2^{\pm}) \\ \eta \end{bmatrix} \\
u = h_u(\bar{x}, v) &= \gamma_2(\xi) + \frac{\partial \psi_1}{\partial \xi_1} \frac{\partial \psi_2}{\partial \xi_2} \psi_3(v, \psi_3^{\pm}(\xi))
\end{aligned} \tag{33}
$$

and the unconstrained system (24a) for the double pendulum on a cart is then given by

$$
\underbrace{\begin{bmatrix} \dot{\xi}_1 \\ \dot{\xi}_2 \\ \dot{\eta}_1 \\ \dot{\eta}_2 \\ \dot{\eta}_3 \\ \dot{\eta}_4 \end{bmatrix}}_{\dot{\bar{x}}} = \underbrace{\begin{bmatrix} \psi_2(\xi_2, \psi_2^{\pm}(\xi_1)) \\ \psi_3(v, \psi_3^{\pm}(\xi)) \\ \eta_2 \\ f_{\varphi_1}(\eta, h_u(\bar{x}, v)) \\ \eta_4 \\ f_{\varphi_2}(\eta, h_u(\bar{x}, v)) \end{bmatrix}}_{\tilde{f}(\bar{x}, v)} . \tag{34}
$$

New unconstrained OCP In view of the change of coordinates (33) and the new dynamics (34), the new unconstrained OCP follows to

$$
\begin{aligned}
\min_{v(\cdot)} \quad & \bar{J}(v) = \int_0^T \Delta\bar{x}^{\mathsf{T}} Q \Delta\bar{x} + R\Delta v^2 + \varepsilon v^2 \, \mathrm{d}t \\
\text{s.t.} \quad & \dot{\bar{x}} = \bar{f}(\bar{x}, v) \\
& \bar{x}(0) = h_x(x_0) , \quad \bar{x}(T) = h_x(x_T) , \quad t \in [0, T]
\end{aligned} \tag{35}
$$

with $\Delta\bar{x} = h_x(\bar{x}) - x_{SP}$ and $\Delta v = h_u(\bar{x}, v) - u_{SP}$.

3.3 Simulation results

The control task for the simulation studies is to perform three successive setpoint changes for the double pendulum starting from an initial state

$$
x_0 = [0\,\mathrm{m}, 0\,\tfrac{\mathrm{m}}{\mathrm{s}}, \pi\,\mathrm{deg}, 0\,\tfrac{\mathrm{deg}}{\mathrm{s}}, \pi\,\mathrm{deg}, 0\,\tfrac{\mathrm{deg}}{\mathrm{s}}]^{\mathsf{T}} \tag{36}
$$

to the desired setpoints

$$
\begin{aligned}
x_{SP1} &= [+0.5\,\mathrm{m}, 0\,\tfrac{\mathrm{m}}{\mathrm{s}}, 0\,\mathrm{deg}, 0\,\tfrac{\mathrm{deg}}{\mathrm{s}}, 0\,\mathrm{deg}, 0\,\tfrac{\mathrm{deg}}{\mathrm{s}}]^{\mathsf{T}} \\
x_{SP2} &= [-0.5\,\mathrm{m}, 0\,\tfrac{\mathrm{m}}{\mathrm{s}}, 0\,\mathrm{deg}, 0\,\tfrac{\mathrm{deg}}{\mathrm{s}}, 0\,\mathrm{deg}, 0\,\tfrac{\mathrm{deg}}{\mathrm{s}}]^{\mathsf{T}} \\
x_{SP3} &= [0\,\mathrm{m}, 0\,\tfrac{\mathrm{m}}{\mathrm{s}}, -\pi\,\mathrm{deg}, 0\,\tfrac{\mathrm{deg}}{\mathrm{s}}, -\pi\,\mathrm{deg}, 0\,\tfrac{\mathrm{deg}}{\mathrm{s}}]^{\mathsf{T}}
\end{aligned} \tag{37}
$$

within the transition times

$$
T_{SP1} = 2.2\,\mathrm{s}, \quad T_{SP2} = 2.0\,\mathrm{s}, \quad T_{SP3} = 2.2\,\mathrm{s} . \tag{38}
$$

The first setpoint realizes a swing-up maneuver of the double pendulum in combination with a side-step over the distance 0.5 m to the right. Next, the double pendulum moves 1 m to the left and finally swings down an moves back to the origin. The limits for the output constraints (25) are set to the values

$$
y_0^{\pm} = \pm 0.65\,\mathrm{m} \quad y_1^{\pm} = \pm 2.0\,\tfrac{\mathrm{m}}{\mathrm{s}}, \quad y_2^{\pm} = \pm 12\,\tfrac{\mathrm{m}}{\mathrm{s}^2} . \tag{39}
$$

The positive definite matrix and the positive scalar in (35) are chosen depending on the desired setpoint according to

$$
\begin{aligned}
Q_{SP1} &= \mathrm{diag}(0, 0, 10, 0, 10, 0), & R_{SP1} &= 1, \\
Q_{SP2} &= 0, & R_{SP2} &= 0.1, \\
Q_{SP3} &= \mathrm{diag}(0, 0, 10, 0, 10, 0), & R_{SP3} &= 1 .
\end{aligned} \tag{40}
$$

A numerical solution of the unconstrained OCP (35) is achieved by solving a two-point boundary value problem (BVP) resulting from the optimality conditions for (35). However, the optimality conditions contain an additional algebraic equation which has to be taken into account. To this end, a modified version of the standard MATLAB solver `bvp4c` is used. The analytical calculation of the coordinate transformation (33), the new system dynamics (34) as well as the optimality conditions are performed with MATHEMATICA and subsequently exported to MATLAB.

Problem (35) is separately solved for all three setpoints (37). Moreover, the penalty parameter is set to $\varepsilon = 10$ as start value and then successively reduced to a final value of $\varepsilon = 10^{-12}$, where the previous solutions are used as initial guess for the next run.

The simulation results for the combined setpoints and for the final value $\varepsilon = 10^{-12}$ are shown in Fig. 3. The two dashed vertical lines in each plot illustrate the trajectories for the setpoints (37) with transition times (38). It can be seen that the output constraints of the double pendulum are satisfied. Moreover, by means of the additionally plotted optimal solution of the constrained OCP (26) it can be observed that the solution of (35) with $\varepsilon = 10^{-12}$ is optimal. Furthermore, the presented results were obtained with asymptotic saturation functions as given in (19).

3.4 Experimental results

The verification of the results is demonstrated on an experimental setup of the double pendulum from the company Hasomed GmbH. The feedforward control computed via solving the unconstrained OCP (35) is implemented in a two-degree-of-freedom control scheme. In order to stabilize the optimal trajectories, a time-varying riccati controller (Kailath, 1980) with high gains on the angles φ_1 and φ_2 is applied. Moreover, a Luenberger observer (O'Reilly, 1983) based on the nonlinear model (1) is used to estimate the cart velocity and the angle rates of both links. The control system is implemented on a dSPACE system with a sampling time of $\Delta t = 1\,\mathrm{ms}$.

The achieved experimental results are also shown in Fig. 3. The trajectories demonstrate that and output constraints (39) are satisfied almost for the entire maneuver. The violation of the constraints is a direct consequence of the control scheme. The additional controller in the closed loop tries to stabilize the double pendulum along the optimal trajectories and therefore causes the resulting control to violate the constraints where it is necessary. This effect is clearly visible for the control u during the time interval $t \in [1, 2]$s. The reason for this behaviour is that the pendulum starts to drift away when approaching the unstable upward position. Therefore, the controller counteracts this effect resulting in higher demands in the feedback part.

4. CONCLUSION

This paper described a transformation method to incorporate constraints in optimal control problems for nonlinear SISO systems. The considered constraints were on the output and a number of its time derivatives. The resulting unconstrained OCP with new system dynamics is fully unconstrained and can therefore be solved with unconstrained optimization methods. The technique was used to compute optimal trajectories for a combined swing-up/swing-down and side-step maneuver of a double pendulum on a cart. The presented simulation and experimental

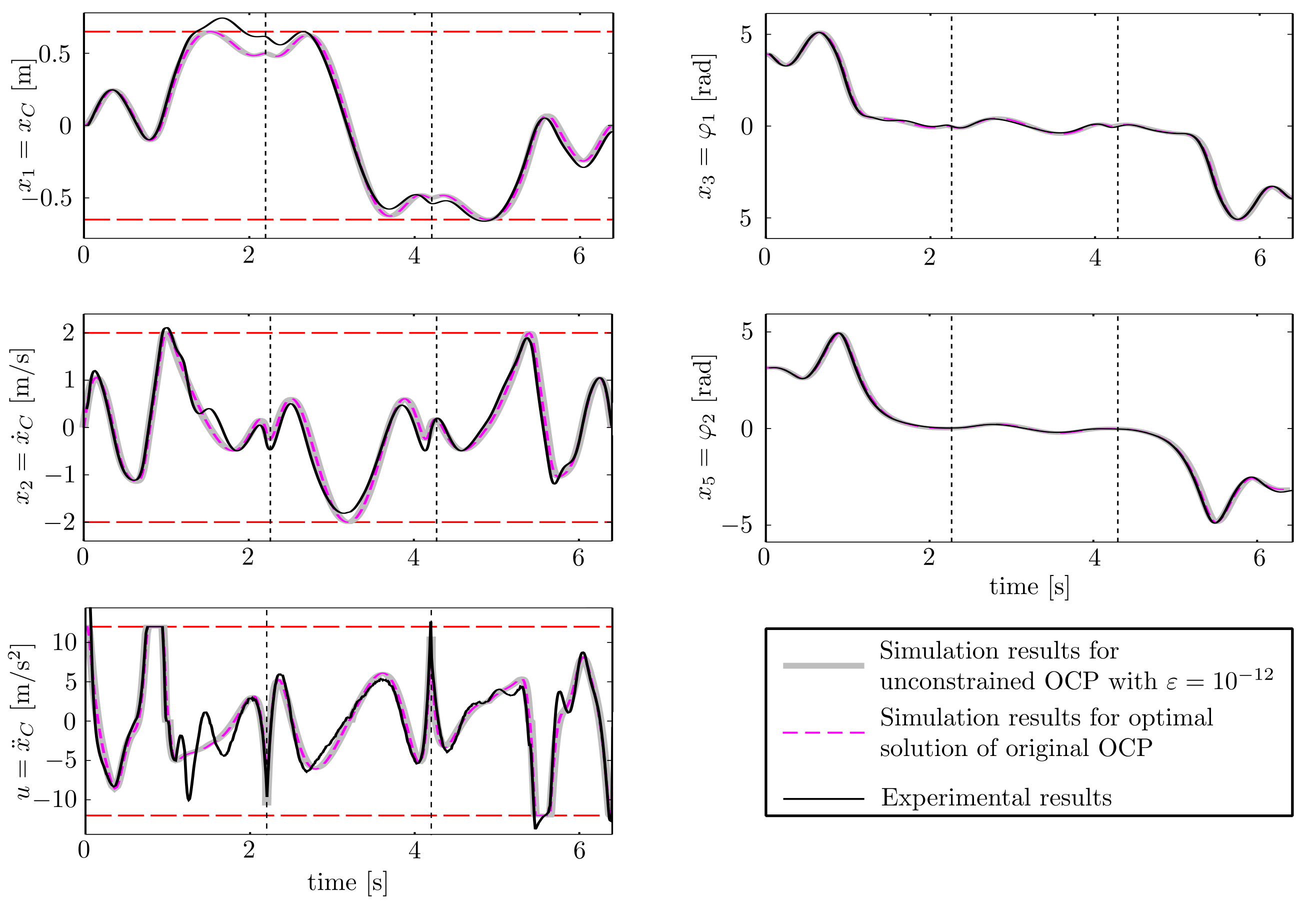

Fig. 3. Simulation and experimental results for the double pendulum on a cart.

results showed the good performance and applicability of the method.

ACKNOWLEDGEMENTS

This work was funded by the Austrian Science Fund (FWF): P21253N22.

REFERENCES

Bryson, A. and Ho, Y.C. (1969). *Applied optimal control*. Ginn & Company.

Bürger, M. and Guay, M. (2010). Robust constraint satisfaction for continuous-time nonlinear systems in strict feedback form. *IEEE Transactions on Automatic Control*, 55(11), 2597–2601.

Graichen, K. and Petit, N. (2009). Incorporating a class of constraints into the dynamics of optimal control problems. *Optimal Control Applications and Methods*, 30(6), 537–561.

Graichen, K., Treuer, M., and Zeitz, M. (2007). Swing-up of the double pendulum on a cart by feedforward and feedback control with experimental validation. *Automatica*, 43(1), 63–71.

Graichen, K. and Zeitz, M. (2008). Feedforward control design for finite-time transition problems of nonlinear systems with input and output constraints. *IEEE Transactions on Automatic Control*, 53(5), 1273–1278.

Hargraves, C.R. and Paris, S.W. (1987). Direct trajectory optimization using nonlinear programming and collocation. *Journal of Guidance, Control and Dynamics*, 10(4), 338–342.

Hasomed GmbH (). *Double pendulum: Product documentation*. Magdeburg, Germany. (www.hasomed.de).

Houska, B., Ferreau, H., and Diehl, M. (2011). An auto-generated real-time iteration algorithm for nonlinear MPC in the microsecond range. *Automatica*, 47(10), 2279 – 2285.

Isidori, A. (1995). *Nonlinear Control Systems*. Springer, Berlin, 3rd edition.

Kailath, T. (1980). *Linear Systems*. Prentice-Hall, Inc., Englewood Cliffs, N.J.

Leineweber, D.B., Bauer, I., Bock, H.G., and Schlöder, J.P. (2003). An efficient multiple shooting based reduced sqp strategy for large-scale dynamic process optimization. part 1: theoretical aspects. *Computers & Chemical Engineering*, 27(2), 157–166.

Nocedal, J. and Wright, S.J. (2006). *Numerical Optimization*. Springer, 2nd edition.

Ohtsuka, T. (2004). A continuation/gmres method for fast computation of nonlinear receding horizon control. *Automatica*, 40(4), 563 – 574.

O'Reilly, J. (1983). *Observers for linear systems*. Academic Press, London.

Wright, S.J. (1997). *Primal-Dual Interior-Point Methods*. Society for Industrial and Applied Mathematics, Philadelphia.